

# Atomic-scale distribution of impurities in CuInSe<sub>2</sub>-based thin-film solar cells

O. Cojocaru-Mirédin<sup>a,\*</sup>, P. Choi<sup>a</sup>, R. Wuerz<sup>b</sup>, D. Raabe<sup>a</sup>

<sup>a</sup> Max-Planck-Institut für Eisenforschung, Max-Planck-Straße 1, 40237 Düsseldorf, Germany

<sup>b</sup> Zentrum für Sonnenenergie- und Wasserstoff-Forschung Baden-Württemberg, Industriestraße 6, 70565 Stuttgart, Germany

## ARTICLE INFO

Available online 11 January 2011

### Keywords:

Thin-film solar cells  
Photovoltaic  
Cu(In,Ga)Se<sub>2</sub>  
CuInSe<sub>2</sub>  
Sodium diffusion  
Grain boundary segregation  
Pulsed laser atom probe  
Transmission electron microscopy

## ABSTRACT

Atom Probe Tomography was employed to investigate the distribution of impurities, in particular sodium and oxygen, in a CuInSe<sub>2</sub>-based thin-film solar cell. It could be shown that sodium, oxygen, and silicon diffuse from the soda lime glass substrate into the CuInSe<sub>2</sub> film and accumulate at the grain boundaries. Highly dilute concentrations of sodium and oxygen were measured in the bulk. Selenium was found to be depleted at the grain boundaries. These observations could be confirmed by complementary energy dispersive X-ray spectroscopy studies. Our results support the model proposed by Kronik et al. (1998) [1], which explains the enhanced photovoltaic efficiency of sodium containing CuInSe<sub>2</sub> solar cells by the passivation of selenium vacancies at grain boundaries.

© 2011 Elsevier B.V. All rights reserved.

## 1. Introduction

Copper indium diselenide (CIS), a compound semiconductor belonging to the I–III–VI<sub>2</sub> chalcopyrite family, is one of the most promising absorber materials for the fabrication of thin-film solar cells. CIS possesses several beneficial material properties such as a direct band gap ( $E_g=1.02$  eV at room temperature), high absorption coefficient ( $\geq 10^5$  cm<sup>-1</sup>), long-term stability, and high radiation hardness [2].

CIS solar cells are commonly deposited on soda lime glass (SLG) substrates, which comprise SiO<sub>2</sub>, Na<sub>2</sub>O, K<sub>2</sub>O, and CaO. Several authors reported diffusion of alkali impurities, in particular sodium, into the CIS film during the processing of these solar cells [3,4]. Interestingly, sodium impurities were found to significantly enhance the photovoltaic conversion efficiency (mainly the open circuit voltage) of CIS solar cells, also known as the “sodium effect” [5,6]. An increase in p-type conductivity [7] and a more pronounced texture (predominance of uniaxial crystallite orientation) [8] were suggested as possible reasons for the enhanced efficiency due to sodium incorporation. However, the “sodium effect” has remained a subject of controversial discussion.

To develop a comprehensive theory of how sodium improves the conversion efficiency of CIS solar cells, one needs to study the elemental distribution at the atomic scale. The concentrations in bulk and grain boundaries are of particular interest. Some attempts have been previously made to determine the impurity concentrations in CIS absorber layers. For instance, Niles et al. [9] applied Auger Electron Spectroscopy (AES) to detect sodium and oxygen segregation at the surface and grain boundaries of CIS and

to show that solute concentrations inside the grains are highly dilute. However, the detection limit of AES for both sodium and oxygen was reported to be only about 0.15 at% [9].

Among the nano-analytical techniques, Atom Probe Tomography (APT) [10–13] is one of the most promising tools for studying solar cells, as it allows for spatially resolved chemical analyses with sub-nanometer resolution [14] and the detection of dilute impurity concentrations as low as a few tens of ppm [15]. First APT results on the elemental distribution in Cu(In,Ga)Se<sub>2</sub> layers, which are similar to CIS, were recently published by Cadel et al. [15] and Schlesiger et al. [16]. Both authors reported significant sodium enrichment at the grain boundaries. The current paper elucidates the atomic-scale elemental distribution in an actual CIS solar cell, using pulsed laser APT. The enhanced energy conversion efficiency due to sodium incorporation is discussed on the basis of the obtained APT results.

## 2. Experimental

A CIS solar cell was fabricated at the Zentrum für Sonnenenergie- und Wasserstoff-Forschung in Stuttgart, Germany. Soda lime glass (SLG) of 3 mm in thickness was used as a substrate material. A Mo back contact layer of 500 nm was deposited onto the SLG substrate by DC sputtering. Subsequently, a polycrystalline CuInSe<sub>2</sub> film of 2 μm in thickness was grown by co-evaporation of the constituent elements using a high temperature single-stage inline process [17]. The substrate temperature during film growth was kept at 600 °C for about 30 min. A CdS buffer layer was deposited by means of chemical bath deposition at 65 °C followed by RF sputtering of an intrinsic ZnO layer, DC sputtering of a ZnO:Al front contact layer, and electron beam evaporation of Ni/Al contact grids.

\* Corresponding author.

E-mail address: o.cojocaru-miredin@mpie.de (O. Cojocaru-Mirédin).

X-ray fluorescence spectrometry (XRF) measurements were performed to determine the overall composition of the CIS layer, using an EAGLE XXL system (0.1 mbar, Si(Li) detector and 50 kV Rh X-ray source). Using the Cu, In, and Se K lines, the accuracy of the calculated concentrations is better than 0.5 at%.

Structural and compositional analyses of CIS films were done by scanning transmission electron microscopy (STEM) and atom probe tomography (APT), respectively. For the STEM investigations, cross-sectional samples were prepared using a dual-beam focused-ion-beam (FIB) (FEI Helios Nanolab 600) and the lift-out technique [18]. STEM was done at a JEOL 2200 FS microscope operated at 200 kV. APT samples were also prepared by means of FIB according to the procedure described in [19,20]. In order to minimize beam damage, a low energy (5 keV) Ga beam was used at the final ion-milling stage. All APT experiments were carried out applying laser pulses of  $\sim 532$  nm wavelength, 12 ps pulse length, and an energy of 0.1 nJ per pulse at a repetition rate of 100 kHz. The specimen base temperature was about 60 K.

### 3. Results and discussion

#### 3.1. Microstructure of the CIS layer

Fig. 1 shows a cross-sectional STEM bright-field image of the studied CIS solar cell, where the stacking sequence of the constituent layers is ZnO:Al/ZnO/CdS/CuInSe<sub>2</sub>/Mo/SLG. The STEM image reveals

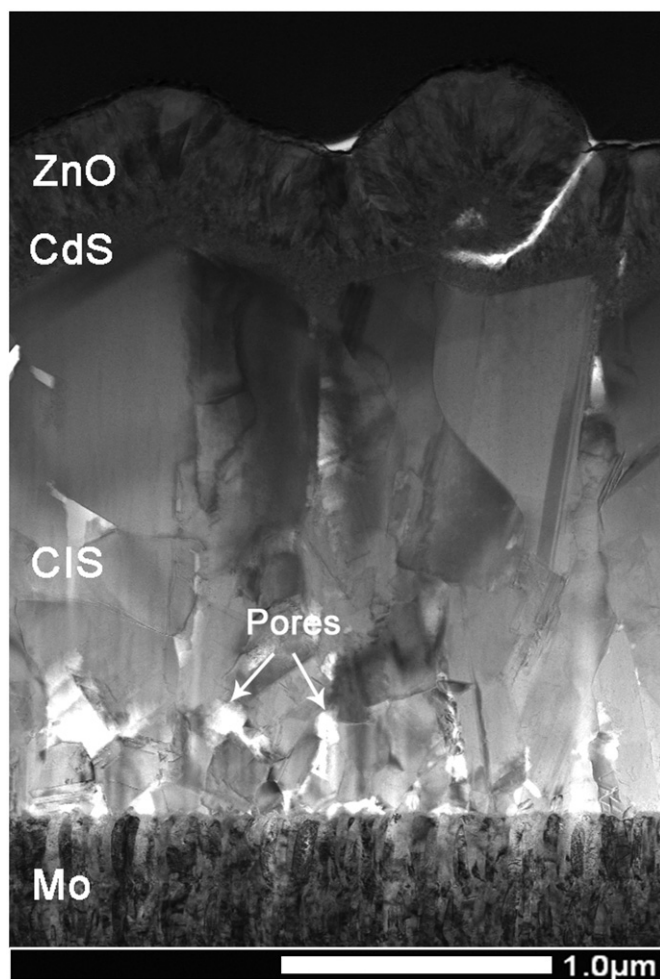


Fig. 1. STEM bright-field image of a CuInSe<sub>2</sub>-based thin-film solar cell in a cross-sectional view.

a polycrystalline CIS layer, which is not smooth but exhibits substantial roughness. Top-view scanning electron microscopy images (not shown here) revealed faceted grains of large size (between 0.7 and 1.25  $\mu\text{m}$ ) and are in agreement with STEM observations. Besides the large grains in the top CIS region, small grains of 0.13 to 0.36  $\mu\text{m}$  in size can be recognized at the bottom of the CIS layer (see Fig. 1). Such a bimodal grain structure is typical of CIS films grown by elemental co-evaporation in the presence of sodium [21] and can be discussed in terms of the van der Drift evolutionary selection mechanism [22]. In this mechanism, the nucleation stage is characterized by randomly oriented nuclei that initially grow independently at uniform rate. In the following stage, the crystals with the direction of fastest growth perpendicular to the substrate are favored over other crystals and will prevail. For a tetragonal crystal, the directions of fastest growth are  $\langle 001 \rangle$ ,  $\langle 100 \rangle$ , and  $\langle 110 \rangle$  [22].

Another interesting feature is the presence of a few voids (about 10 to 100 nm in size) in the CIS layer close to the CIS/Mo interface (see Fig. 1). These voids probably stem from the deposition process and are not formed during TEM sample preparation, as the sample was finally ion-milled at only 5 kV. Such nano-voids in the CIS layer were also observed by Lei et al. [23] and for CIGS layers by Rudmann [24].

#### 3.2. Composition of CIS layer (grain and grain boundary)

A typical mass spectrum obtained from an APT analysis of a CIS layer is given in Fig. 2. While copper and indium were detected as both single and double charged ions, selenium ions were only detected in a single charged state. Complex ions, namely  $\text{CuCO}^+$ ,  $\text{CuSe}^+$ ,  $\text{Cu}_2\text{Se}^+$ ,  $\text{CuSe}_2^+$ ,  $\text{Se}_2^+$ , and  $\text{Se}_3^+$  were detected as well. Sodium was detected as  $\text{Na}^+$ . The background noise level in the mass range close to the  $\text{Na}^+$  peak is extremely low ( $\approx 40$  ppm/a.m.u.) so that even very low dilute sodium concentrations can be detected. Besides sodium, oxygen and silicon impurities were detected as  $\text{O}^+$ ,  $\text{O}_2^+$ ,  $\text{Si}^{2+}$ , and  $\text{Si}^+$ . A small amount of  $\text{Ga}^+$  was also detected.

Fig. 3 shows three-dimensional maps of all the detected elements as well as sodium and oxygen only. The analyzed volume is about  $120 \times 120 \times 390$  nm<sup>3</sup> in size and represents the interior of a CIS grain. The measured bulk composition is  $23.4 \pm 0.06$  at% Cu,  $29.0 \pm 0.07$  at% In, and  $47.4 \pm 0.08$  at% Se, which is in good agreement with the integral XRF measurement (compare APT-1 and

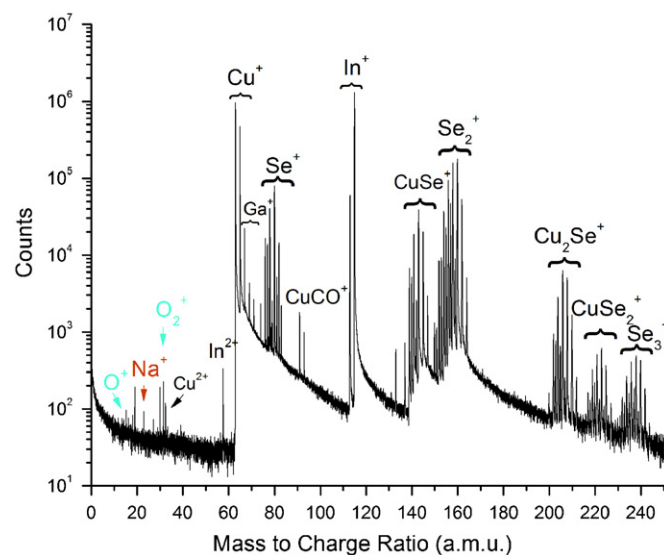


Fig. 2. Mass spectrum of the complete measurement from Fig. 3 with details showing the minority elements (Na and O) in the low mass region.

Download English Version:

<https://daneshyari.com/en/article/1677985>

Download Persian Version:

<https://daneshyari.com/article/1677985>

[Daneshyari.com](https://daneshyari.com)